

Anomalous photocurrent transients in nematic liquid crystals: The nonlinear optical Pockel's effect induced by the Fréedericksz transition

Akihiko Sugimura

Department of Information Systems Engineering, Faculty of Engineering, Osaka Sangyo University, Nakagaito, Daito, Osaka 574, Japan

Ou-Yang Zhong-can

Institute of Theoretical Physics, Academia Sinica, P.O. Box 2735, Beijing 100 080, China

(Received 17 January 1991)

The mechanism of the normally incident photoinduced current transients in homogeneous nematic samples in an applied dc voltage has been studied theoretically and experimentally. Explicit expressions for the photovoltaic emf are derived using the nonlinear optical Pockel's effect induced by the Fréedericksz transition. The current transient is elucidated by the effect of dc field-induced ion drift to electrodes based on an equivalent circuit. The experimental results [briefly reported in *Phys. Rev. Lett.* **63**, 555 (1989)] are completely explained by the present theory. According to the theoretical prediction, two methods to enhance the photoinduced current in liquid crystals, light exposure and dye doping, have been found and implemented.

PACS number(s): 61.30. -v, 72.40. +w

I. INTRODUCTION

Recently we have reported on the anomalous photoinduced current transients (APCT) in a nematic liquid crystal (NLC) 4-cyano-4'-alkyl-biphenyls (5CB) [1]. A nonlinear optical mechanism was also suggested for the APCT effect [2,3]. The fundamental interest and potential application to liquid-crystal (LC) neutral-network devices [4] motivated us to investigate this problem in greater detail. In this paper, recent extensive study in both theory and experiment is reported. As shown in the following sections, the APCT can be described as an optical rectification of the NLC by the nonlinear optical Pockel's effect induced by the Fréedericksz transition.

It is well known that the linear optical dielectric tensor $\epsilon(\omega)$ of an anisotropic medium is a function of \mathbf{E}_{app} in the presence of an applied dc field \mathbf{E}_{app} :

$$\epsilon(\omega) = \epsilon^{(0)}(\omega) + \epsilon^{(1)}(\omega) \cdot \mathbf{E}_{\text{app}} + \cdots \quad (1)$$

This is generally called Pockel's effect. For a nonlinear optical medium, the nonlinear electric polarization \mathbf{P}^{NL} induced by incident light may be written in the form [5]

$$P_i^{\text{NL}}(\omega) = \sum_{\omega_m} \chi_{ijk} E_j(\omega_m) E_k(\omega - \omega_m) + \sum_{\omega_m} \chi_{ijkl} E_j(\omega_m) E_{l,k}(\omega - \omega_m) + \cdots, \quad (2)$$

where $E_j(\omega)$ is the j th component of the optical field, $E_{l,k} = \partial E_l / \partial x_k$ and χ_{ijk} are the nonlinear optical susceptibilities. Here and in the following the summation convention is used. In Eq. (2) the nonlinear electric polarization \mathbf{P}^{NL} may include two kinds of nonlinear optical processes. One is related to the sum-frequency generation. The second-harmonic generation (SHG) is such an exam-

ple. The other is related to the difference-frequency generation. Optical rectification is an example of the latter case. Because an aligned NLC possesses $D_{\infty h}$ symmetry, its nonlinear optical susceptibilities χ_{ijk} vanish. In the presence of an applied dc field \mathbf{E}_{app} , however, a transition from a uniform to an elastically deformed state can occur in the aligned NLC [6]. This is the well-known Fréedericksz transition. By this deformation, NLC macroinversion symmetry may be broken. If so, the third-order tensor χ_{ijk} emerges and depends on \mathbf{E}_{app} . To be consistent with Pockel's effect in linear optics shown in Eq. (1), we call this effect the nonlinear optical Pockel's effect induced by the Fréedericksz transition (NOPF effect) in NLC. In the following the mechanism of the observed APCT in 5CB will be shown to be because of this effect. In Sec. II we briefly state the experimental methods. In Sec. III the theory of the NOPF effect as well as the associated APCT are outlined. For the latter we introduce an equivalent circuit to account for the effect of dc field-induced ion drift to electrodes of the NLC cell. In Sec. IV the experimental results, including some new ones, are summarized and compared with theory. In Sec. V, the behavior of the NOPF effect in nematic-isotropic (NI) phase transition and a dielectric-anisotropy dependence of the APCT are discussed. In particular, two methods that enhance the NOPE and the APCT in NLC are presented. These methods were first suggested by theory and then implemented in our experiment. Finally, Sec. VI concludes the paper.

II. EXPERIMENTAL SETUP

Figure 1 shows our experimental setup. The nematic liquid-crystal material was introduced between two pieces of glass with transparent In_2O_3 electrodes on their sur-

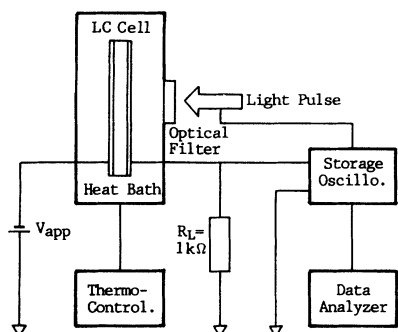


FIG. 1. Experimental setup.

faces. The area of these cells is typically 2 cm^2 . The thickness of one type of the cell is $d = 6.8$ and $28 \mu\text{m}$ for another type. The material used is 5CB (BDH Chemical Ltd., K15), which has a positive dielectric anisotropy ($\Delta\epsilon = 10$). The substrate surfaces were unidirectionally rubbed in an antiparallel manner to produce homogeneous nematic molecular alignment. The molecular alignment of both types of cell was checked by orthoscopic observation with a microscope. The samples were illuminated perpendicularly by a depolarized xenon-flash-lamp pulse (for example, energy $15 \mu\text{J}/\text{cm}^2$, duration 10

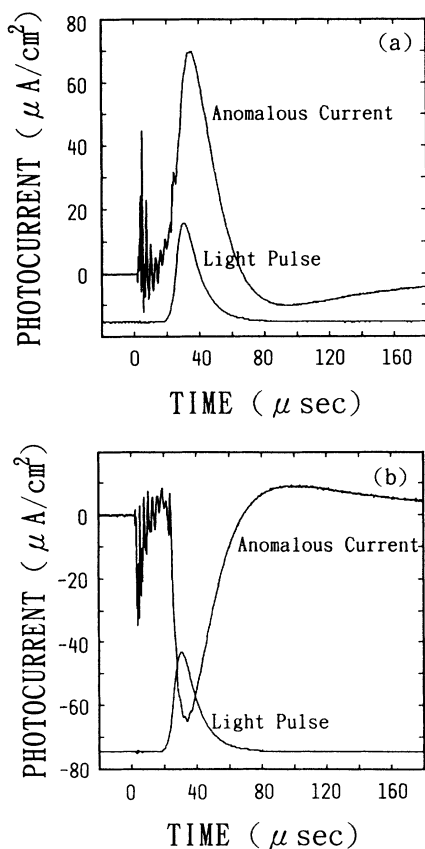


FIG. 2. Typical current transients of 5CB sample at a constant temperature of 30°C , across which (a) a negative voltage of -30 V is applied, and (b) a positive voltage of $+30 \text{ V}$ is applied.

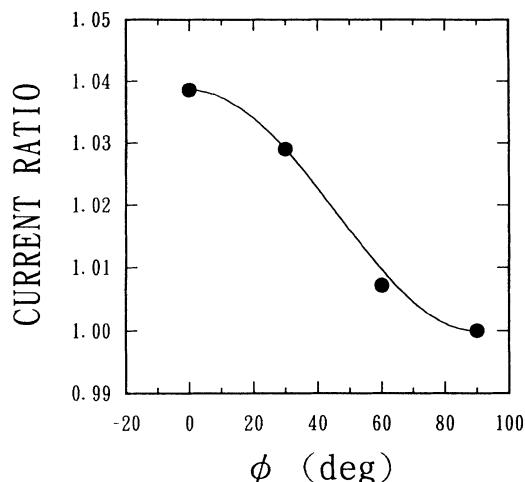


FIG. 3. Photoinduced current dependence of light polarization. Current ratio means the normalized value of $I_p(\phi)/I_p(90^\circ)$.

μsec). The energy of the light pulse was monitored by using a joulemeter (Gentec Inc., ED-100A). A stabilized dc voltage V_{app} was applied across the cells to cause the deformation of LC. Transient currents were observed through a series load resistor ($1 \text{ k}\Omega$) by means of a digital storage oscilloscope (Iwatsu DS-8621). The measured signal was also sent to a microcomputer to draw and display directly the transient current shape (Fig. 2). Interference filters ($\lambda_{\text{max}} = 350, 400, 450, 500, 550, 600, 650, 700, 750, 800, 850, 900 \text{ nm}$) were used for the measurements of the spectral sensitivity. In addition to the use of depolarized light, a linear polarizer was used to measure the polarized sensitivity of the APCT. This result (Fig. 3) was not reported in our previous Letter [1]. To test the dielectric-anisotropy dependence of APCT a mixture of nematic azoxy compounds and a biphenyl ester (Merck Ltd., 997DSM Licristal) having $\Delta\epsilon = -0.6$ was investigated. The APCT of dye-doped 5CB was also measured and a great enhancement of APCT in this sample was observed. After the theoretical discussions in the next section, this enhancement effect will be discussed.

III. THEORY

The evidence of nonlinear optical mechanism of APCT and NLC comes from two facts in the experiment [1]: (i) The magnitude of APCT peaks increases linearly with the intensity of illuminated light, which is proportional to the square of the magnitude of the optical electric field, and (ii) the response time for the first APCT peak is fast, of the order of microseconds, and is independent of the applied bias dc field. Both facts seem to reject the transport mechanism of photogenerated or photopyroelectric ions in LC. The typical response time of ion transport in LC is of the order of $10\text{--}100 \text{ msec}$ and has to vary with applied voltage (see below). Based on a continuum model of NLC, the theory of nonlinear optics in NLC with good alignment or with curvature stains has been previously established for SHG in LC [7]. The present theory basically follows the comment [2] in which the two peaks of

APCT have been briefly explained as the photovoltaic effect of the nonlinear polarization together with the dc field-induced ion drift to electrodes, i.e., the electric double-layer effect. The detailed mechanism for the photovoltaic effect in APCT and NLC has been further clarified. As shown in Eq. (2), the nonlinear source P^{NL} has two contributions. The second term of Eq. (2),

$$P_i^{NL}(0) = \chi_{ijkl}(0 = \omega - \omega) E_j(\omega) E_{l,k}(\omega), \quad (3)$$

plays a dominant role in nonlinear optics for an aligned NLC. In Appendix A we will show that its contribution may reduce to the effect that it can combine into the first term of Eq. (2) as a weaker part. The polarized direction of P^{NL} in Eq. (3) has to depend on the incident direction of the light. This effect, however, cannot be verified by our recent experimental check and will be explained in Appendix A. In fact, when an applied dc voltage is converse and the incident light is kept in the same direction, the same converse for APCT but no change in shape [see Figs. 2(a) and 2(b)] is observed. It is easy to see that this experimental result is equivalent to the fact that the APCT is independent of the incident direction of the light. Therefore the photovoltaic effect for APCT in NLC is now considered only as a NOPF effect:

$$P_i^{NL}(0) = \chi_{ijk}(0 = \omega - \omega, \mathbf{E}_{app}) E_j(\omega) E_k(\omega). \quad (4)$$

A. Fréedericksz transition in the asymmetric cell

To derive the NOPF tensor $\chi_{ijk}(\mathbf{E}_{app})$ we first study the distortion of NLC induced by electric fields; in particular, with the planar orientation and with positive dielectric anisotropy. Although the problem has been considered by several authors [8], it is important to note that these studies are performed in two extreme cases either with a conducting nematic sample or an insulating nematic sample. The distortion in a practical NLC layer is more complicated by the fact that the electric field is in general not symmetric with respect to the midplane of the cell as required in both extreme cases. Experiment [9] demonstrated that for a NLC sample the field at the anode is at least ten times higher than the average field. The effect at the cathode, however, becomes much smaller. The reason in this example is that, in the cell, the negative and positive space charges (ions and others) have different mobility and the electric double layers are formed by field-induced ion drift to both electrodes in different ways. A complete quantitative study on this phenomenon appears difficult because it involves many chemical and physical processes [10]. In our theoretical treatment an equivalent circuit shown in Figs. 4(a) and 4(b) is assumed to account for the asymmetry of field, where R_e and C_e are the resistance and capacitance of the electric double layers near the electrodes (especially for the anode), respectively, and R_o and C_o are those of bulk of the cell [11], respectively. At the equilibrium, the double layers decrease the effective applied dc voltage, affecting the distortion of the NLC, which is given by

$$V_{eff} = V_{app} R_o / (R_o + R_e). \quad (5)$$

The energy of the light pulse used in our experiment is of

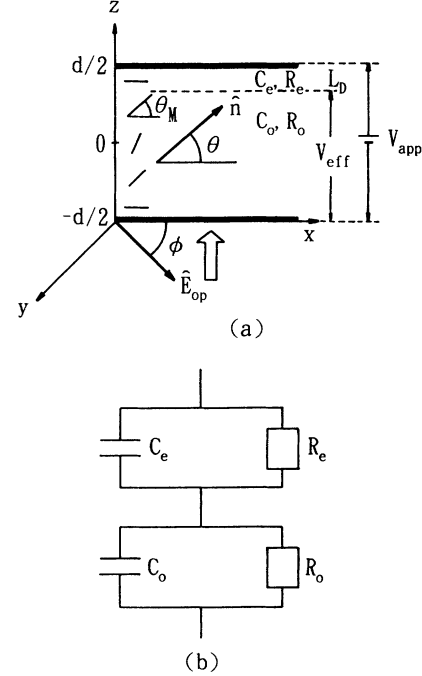


FIG. 4. (a) Geometry of nonlinear optical Pockel's effect induced by the Fréedericksz transition in a planar parallel oriented NLC cell. (b) Equivalent circuit of a NLC cell allowing for an electrical double layer.

the order of $\mu J/cm^2$, so it will not be necessary to consider the reorientation effect by the light. The total free energy of the system F contains two terms associated with elastic distortion and with interaction of the LC with field V_{eff} ,

$$F = F_f + F_e. \quad (6)$$

F_f is the Frank free energy [12] given by

$$F_f = \frac{1}{2} \int \{ K_1 (\nabla \cdot \mathbf{n})^2 + K_2 (\mathbf{n} \cdot \nabla \times \mathbf{n})^2 + K_3 [\mathbf{n} \times (\nabla \times \mathbf{n})]^2 \} dv. \quad (7)$$

K_1 , K_2 , and K_3 are the splay, twist, and bend elastic constants of NLC and \mathbf{n} is the director. In the geometry shown in Fig. 4(a), the director may be expressed as

$$\mathbf{n} = (\cos\theta, 0, \sin\theta). \quad (8)$$

The distorted angle θ is a function of z . The energy of the field related to the distortion of LC is

$$F_e = -\frac{\Delta\epsilon}{8\pi} \int (\mathbf{E}_e \cdot \mathbf{n})^2 dv. \quad (9)$$

In general \mathbf{E}_e is not uniform across the sample. However, when the influence is considered in R_e and C_e , the field given by

$$\mathbf{E}_e = \frac{V_{eff}}{d} (0, 0, 1) \quad (10)$$

is not so far away from reality [9]. By this treatment it is not necessary to assume that the LC is either insulating

or conducting. Another simplification that greatly facilitates the mathematics is setting

$$K_1 = K_2 = K_3 = K. \quad (11)$$

The total free energy per unit area is now obtained by [13]:

$$G = F/A_0 = \frac{1}{2}K \int_{-d/2}^{d/2-L_D} \left[\left(\frac{d\theta}{dz} \right)^2 - \xi^{-2} \sin^2\theta \right] dz, \quad (12)$$

where A_0 is the area,

$$\xi = (d - L_D) \sqrt{4\pi K} / (V_{\text{eff}} \sqrt{\Delta\epsilon}),$$

and L_D is the double-layer thickness. The energy has a minimum value when $\theta(z)$ satisfies

$$\int_{-d/2}^z dz = \xi \int_{\theta_1^0}^{\theta(z)} d\theta \frac{1}{(\sin^2\theta_M - \sin^2\theta)^{1/2}}, \quad (13)$$

where θ_1^0 is the tilt angle of the NLC director at the surface of $z = -d/2$ (the tilt angle at $z = d/2 - L_D$ will be denoted as θ_2^0), and the extreme distortion angle θ_M occurring at z_M may be determined by solving the two equations

$$z_M + \frac{d}{2} = \xi \int_{\theta_1^0}^{\theta_M} d\theta \frac{1}{(\sin^2\theta_M - \sin^2\theta)^{1/2}}, \quad (14)$$

$$\frac{d}{2} - L_D - z_M = \xi \int_{\theta_2^0}^{\theta_M} d\theta \frac{1}{(\sin^2\theta_M - \sin^2\theta)^{1/2}}. \quad (15)$$

$$\begin{aligned} \chi_{ijk} = & B_1 b_i n_j n_k + B_2 n_i b_j n_k + B_3 n_i n_j b_k + B_4 (\nabla \cdot \mathbf{n}) n_i n_j n_k + B_5 b_i \delta_{jk} + B_6 \delta_{ij} b_k + B_7 \delta_{ik} b_j \\ & + B_8 (\nabla \cdot \mathbf{n}) n_i \delta_{jk} + B_9 (\nabla \cdot \mathbf{n}) \delta_{ij} n_k + B_{10} (\nabla \cdot \mathbf{n}) \delta_{ik} n_j + B_{11} n_i n_{k,j} + B_{12} n_i n_{j,k} + B_{13} n_j n_{i,k} \\ & + B_{14} n_j n_{k,i} + B_{15} n_k n_{i,j} + B_{16} n_k n_{j,i}, \end{aligned} \quad (19)$$

where

$$\mathbf{b} = \mathbf{n} \cdot \nabla \mathbf{n}, \quad n_{i,j} = \frac{\partial n_i}{\partial x_j}, \quad (20)$$

and $B_1 - B_{16}$ are the material constants dependent upon the physical processes and mechanism.

Inserting Eq. (8) into Eqs. (19) and (20), we can get a simpler form of the tensor in terms of $\theta(z)$ and $d\theta/dz$. With the help of Eqs. (13) and (18) the NOPF's tensor $\chi(V_{\text{app}})$ can then be obtained. However, our interest is the nonlinear optical polarization associated with the NOPF effect and we therefore omit giving the heavy formula for $\chi(V_{\text{app}})$. We give directly $\mathbf{P}^{\text{NL}}(V_{\text{app}})$. If polarized light of frequency ω_0 is normally incident on the LC cell, the optical field is given by

$$\mathbf{E}_{\text{OP}}(z, \omega) = E_{\text{OP}}(z, \omega) (\cos\phi, \sin\phi, 0), \quad (21)$$

ϕ being the polarized angle from the x axis [see Fig. 4(a)]. Based on Lambert's law of absorption we have

Because the field at the anode is much higher than the average field and L_D is always less than $1 \mu\text{m}$ [11], *in situ* we may set $\theta_M = \theta_2^0$ (i.e., $z_M = d/2 - L_D$). From Eqs. (5) and (13)–(15) one can only find a critical applied voltage,

$$V_{\text{app}}^c = \frac{1}{2}(1 + R_e/R_0) \pi \sqrt{4\pi K / \Delta\epsilon}, \quad (16)$$

under the condition of $\theta_1^0 = 0$. The transition of the NLC at the critical voltage from the undistorted state to the distorted one is the well-known Fréedericksz transition. Above V_{app}^c , Eqs. (14) and (15) may reduce to

$$\frac{V}{V_{\text{app}}^c} = \frac{2}{\pi} \int_0^{\pi/2} d\theta \frac{1}{(1 - \sin^2\theta_M \sin^2\theta)^{1/2}}. \quad (17)$$

By expanding the integral function we obtain the result

$$\frac{V}{V_{\text{app}}^c} - 1 = \frac{1}{4} \sin^2\theta_M + \dots \quad (18)$$

This formulation allows us to determine the extreme distorted angle θ_M with the applied dc voltage V_{app} and will serve to give the expression of the nonlinear optical Pockel's effect in the following subsection.

B. NOPF polarization

In the continuum theory of NLC, the director $+\mathbf{n}$ and $-\mathbf{n}$ are considered as equivalent to each other. By keeping only the first order of deformation terms $\nabla \mathbf{n}$ it has been proved [7] that the most general form of third-order tensors independent of the detailed mechanisms in a distorted NLC is

$$E_{\text{OP}}(z, \omega) = E_0 e^{-\beta(z+d/2)/2} (\delta_{\omega, \omega_0} e^{iqz} + \delta_{\omega, -\omega_0} e^{-iqz}), \quad (22)$$

where parameter β is the attenuation coefficient of the LC, q is the wave number, and E_0 is the initial magnitude of the optical field. With Eqs. (4), (8), and (19)–(22), a straightforward calculation gives the nonlinear optical polarization along the z axis,

$$\begin{aligned} P_z^{\text{NL}}(z, \omega = 0) = & E_0^2 e^{-\beta(z+d/2)} \cos\theta \\ & \times \sin\theta [A + \cos^2\phi (B + C \sin^2\theta)] \frac{d\theta}{dz}, \end{aligned} \quad (23)$$

with $A = B_5$, $B = B_8 + B_1 - B_4 - B_{14} - B_{16}$, and $C = B_4 - B_1 - B_2 - B_3$. For the case of depolarized light one simply replaces $\cos^2\phi$ by $\frac{1}{2}$.

C. Photorectification and APCT

To simplify the computation, in the preceding subsection it was assumed that the light beam intensity can be

approximated as uniform over the cell surface, i.e., as independent of x and y coordinates. Following this approximation, the photovoltaic or photorectification effect caused by the nonlinear optical polarization (OP) may be represented as an additional emf U_{OP} across the NLC layer given by

$$U_{\text{OP}} = 4\pi \int_{-d/2}^{d/2-L_D} P_z^{\text{NL}}(z, \omega=0) dz, \quad (24)$$

where we omit the contribution of the double layer for $L_D \ll d$. Inserting Eq. (23) into Eq. (24) and taking the partial integration for the obvious angle-dependent terms we get

$$U_{\text{OP}}^b = \pi\beta E_0^2 \int_{-d/2}^{d/2-L_D} e^{-\beta(z+d/2)} \sin^2\theta [2A + \cos^2\phi(2B + C \sin^2\theta)] dz. \quad (27)$$

Accordingly, the term U_{OP}^s is the component of U_{OP} that depends only on the polarized direction of V_{app} but does not depend on the incident-light direction. The second term U_{OP}^b may be regarded as the bulk absorption contribution of the NLC layer. With the midvalue theorem of the integral, the latter may be evaluated as

$$U_{\text{OP}}^b = \pi\alpha\beta(d-L_D)E_0^2 e^{-\beta(d/2-L_D)} \times \sin^2\theta_M [2A + \cos^2\phi(2B + C \sin^2\theta_M)], \quad (28)$$

where θ_M is the deformed angle at $z=d/2-L_D$. The magnitude of the integral factor α is near 1. Considering the approximation of Eq. (18) we have the expression U_{OP}^b similar to U_{OP}^s by

$$U_{\text{OP}}^b = 8\pi\alpha\beta(d-L_D)E_0^2 e^{-\beta(d/2-L_D)} \left[\frac{V_{\text{app}}}{V_{\text{app}}^c} - 1 \right] \times \left\{ A + \cos^2\phi \left[B + 2C \left[\frac{V_{\text{app}}}{V_{\text{app}}^c} - 1 \right] \right] \right\}. \quad (29)$$

Clearly, the sign of U_{OP}^b should depend on the direction of the incident light. Because $\alpha\beta d \ll 1$; however, we always have $|U_{\text{OP}}^b| < |U_{\text{OP}}^s|$. In other words, the sign of U_{OP} is determined not only by the polarized direction of V_{app} but by that of the incident light. This theoretical result does agree with experimental observations as shown in Figs. 2(a) and 2(b). On the other hand, there is a little difference in the magnitude of APCT between Figs. 2(a) and 2(b) upon a close inspection. This difference can be revealed by the contribution of U_{OP}^b . Because $E_0^2 \propto I_0$, where I_0 is the intensity of the incident beam, the last two formulations show clearly what is meant by the NOPF's effect.

Based on these theoretical treatments and the equivalent circuit of NLC [Fig. 4(b)], the calculation of the photoinduced current transients is a straightforward matter. Before getting into the actual calculation we note from experiment [9] that the extent of the electric double

$$U_{\text{OP}} = U_{\text{OP}}^s + U_{\text{OP}}^b, \quad (25)$$

where with the $\theta_1^0=0$ and $\theta_2^0=\theta_M$,

$$U_{\text{OP}}^s = E_0^2 \pi \{ e^{-\beta d} \sin^2\theta_2^0 [2A + \cos^2\phi(2B + C \sin^2\theta_2^0)] - \sin^2\theta_1^0 [2A + \cos^2\phi(2B + C \sin^2\theta_1^0)] \} \\ = 8\pi E_0^2 e^{-\beta d} \left[\frac{V_{\text{app}}}{V_{\text{app}}^c} - 1 \right] \\ \times \left\{ A + \cos^2\phi \left[B + 2C \left[\frac{V_{\text{app}}}{V_{\text{app}}^c} - 1 \right] \right] \right\}, \quad (26)$$

and

layer, mainly occurring at the anode, is not more than 10% of the bulk thickness. Based on a preliminary consideration for a two-plane capacitor ($C \propto 1/l$ where l is the distance of two planes) it is clear that the capacitance of the electric double-layer C_e is large in comparison with that of bulk C_0 . So in our previous calculation [2], C_0 is neglected. Furthermore, as shown in Fig. 2 we simplify the incident-light pulse by a Dirac function $I_0\delta(t/\tau_0)$, where τ_0 is the duration of the pulse. Then the photoinduced current transient I_p is obtained (see Appendix B) by

$$I_p = \frac{U_{\text{OP}}}{R_0} \left[\delta \left[\frac{t}{\tau_0} \right] - \frac{\tau_0}{R_0 C_e} \exp \left[-\frac{t}{\tau} \right] \right], \quad (30)$$

where

$$\tau = \frac{R_0 R_e C_e}{R_0 + R_e}. \quad (31)$$

The two peak current transients observed in experiment can be well explained by this expression both in sign and in shape. In the following section, we give more detailed comparisons of experimental results with theory.

IV. COMPARISON WITH EXPERIMENT

A. Threshold voltage

Because the cells used in our experiment were treated as a homogeneous alignment, threshold phenomenon should exist. In both insulating and conducting extreme cases, the threshold voltage V_c of the Fréedericksz transition in the splay mode is $\pi(4\pi K/\Delta\epsilon)^{1/2}$. In our present theory, shown in Eq. (16), however, the threshold value increases by a factor $\frac{1}{2}(1+R_e/R_0)$. This was found to be true qualitatively. Necessary physical constants of 5CB at temperatures near 30°C are set by $K=7.20 \times 10^{-7}$ dyn (at $T=26^\circ\text{C}$) and $\Delta\epsilon=\epsilon_{\parallel}-\epsilon_{\perp}=17.1-7.2=9.9$ (at $T=29^\circ\text{C}$) from a previous measurement [14] and other

data [15], respectively, and therefore $V_c = 0.89$ V from the above formula. By extrapolating the $I_p - V_{app}$ curve shown in Fig. 2 of our Letter [1], we obtained the experimental threshold voltage $V_{app}^c = 1.5$ V.

B. $I_p - V_{app}$ characteristics

The detailed relationship between the photoinduced current and the applied dc voltage, i.e., the $I_p - V_{app}$ characteristics for the cell of $d = 6.8$ μm can be found in Fig. 2 of Ref. [1]. As pointed out previously, the magnitudes of the first peak and the second peak of the photocurrent transient yield the same relation of $I_p \propto (V_{app} - V_{app}^c)^n$, where the exponent n is about 2.0 for lower V_{app} and approaches 1.0 at higher voltages. These characteristics confirm our theoretical predictions shown in Eqs. (26), (29), and (30). The decrease of the value of n with the increase of V_{app} is in agreement with the saturation feature of the $\theta_M - V_{app}$ characteristic curve of the Fréedericksz transition at higher voltages (see, for example, Fig. 8 on p. 118 of Ref. [13]).

C. Response times

A direct and simple check for the present theoretical model can be made from the measurement of the transient photoinduced current. Equations (30) and (31) show that each response time τ_0 and τ for the two peaks of the current transient are obviously different in relationship to the applied dc voltage. The response time τ_0 is also the duration of the incident-light pulse as defined in Sec. III C and, of course, is independent of V_{app} , as we have pointed out [1]. On the other hand, response time τ is proportional to $C_e R_e$, which is the characteristic time of the field-induced electric double layer near the electrode. Therefore the response time τ has to change with the applied dc voltage V_{app} . We have carried out the measurement to check the above prediction. The result (shown in Fig. 5) shows good agreement.

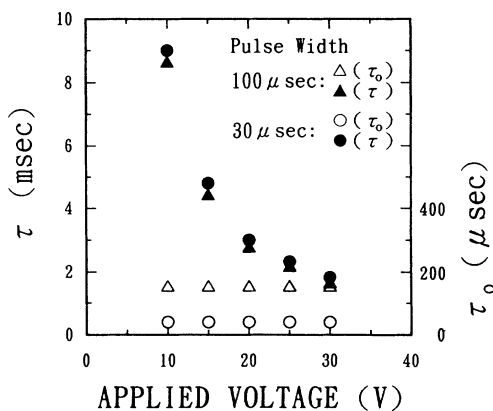


FIG. 5. Different dependences of two response times τ_0 and τ on the applied dc voltages for two different light pulses of 30 μsec (circular symbols) and 100 μsec (triangular symbols).

D. Dependence of light polarization

The present theory can be checked by measuring the APCT dependence of light polarization. This experiment has been carried out at $V_{app} = 30$ V. Figure 3 shows the measured I_p as a function of light-polarized angle ϕ . This result appears to some extent in the characteristic shown in Eqs. (26) and (29). The very weak relationship between I_p and ϕ is borne out of the theory that at a higher applied voltage, the distortion of the NLC director has to be near the saturation state in which the NLC directors are near normal to the surfaces of the cell. In other words, the cell now has somewhat cylindrical symmetry with respect to the incident light.

E. Spectral sensitivity

Another piece of evidence is obtained by measuring the spectral sensitivity of the APCT. A preliminary result observed in the $d = 6.8$ μm cell of 5CB was set in Fig. 3 in our Letter [1]. Again comparing the sensitivity curves of two peaks currents ($V_{app} = -30$ V and $T = 30^\circ\text{C}$) with the spectral absorbance of the LC, we see that all three curves are linearly related to each other. The reason for this is clearly due to both contributions described in Eqs. (26) and (29), related to the absorption coefficient β . The latter characterizes the spectral absorbance of the medium. In our previous Letter, we were mistaken that the first-peak current is almost independent of the wavelength. This mistake was caused by identifying the first-peak current as anomalous and the second-peak current as the normal one. From a present reconfirmation, in fact both peaks of APCT are due to the same mechanism, as expressed in Eqs. (26) and (29).

V. FURTHER DISCUSSION

A. $\Delta\epsilon$ dependence

In the preceding section, we have compared in detail the experimental results with theoretical predictions and found good agreement. However, there are two observed characteristics that have not yet been explained: the dependence of the APCT on a dielectric-anisotropy $\Delta\epsilon$ and the anomalous behavior of the APCT in the vicinity of the nematic-isotropic (NI) phase transition. As reported in our Letter [1], we used the 997DSM LC with negative $\Delta\epsilon$ instead of 5CB, and found that the photocurrent changes its direction at the same polarization of V_{app} . A direct study of the mechanism of the NOPF's coefficients $B_1 - B_{16}$ may give the answer to this problem. For example, in the SHG theory of NLC [7], with special consideration of the contribution of the flexoelectric effect of LC, it was shown that some B_i 's may be expressed by [(4.25) of Ref. [7]]:

$$\chi' = \frac{\Delta\epsilon(\omega)[e_{33}(\omega') - e_{11}(\omega')]}{4\pi(I\omega'^2 + i\gamma_1\omega')}, \quad (32)$$

where new parameters e_{11} and e_{33} are the flexoelectric coefficients, and I and γ_1 are the moment of inertia of the π electrons per unit volume of the NLC and the light dis-

sipative constant, respectively. Specifying the present photorectification in Eq. (32), we should set $\omega=0$ and $\omega'=\omega_0$ (the incident-light frequency). So the dependence of I_p on $\Delta\epsilon$ can be explained by the flexoelectric effect. But the B_1-B_{16} may not only come from the contribution of flexoelectric effect; therefore in the following we will give a more general consideration to understanding this problem.

In the SHG theory of LC it was shown that for an aligned sample, the fourth-order tensor of NLC may in general be written as [Eq. (28) of Ref. [7]]

$$\begin{aligned} \chi_{ijkl} = & A_1 n_i n_j n_k n_l + A_2 n_i n_j \delta_{kl} + A_3 n_i n_k \delta_{jl} \\ & + A_4 n_i n_l \delta_{jk} + A_5 n_k n_l \delta_{ij} + A_6 n_j n_k \delta_{il} \\ & + A_7 n_j n_l \delta_{ik} + A_8 \delta_{ij} \delta_{kl} \\ & + A_9 \delta_{ik} \delta_{jl} + A_{10} \delta_{il} \delta_{jk} . \end{aligned} \quad (33)$$

The NOPE's third-order tensor χ_{ijk} shown in Eq. (19) can be forward generated by inserting the operator ∇_l

$$\begin{aligned} \chi'_{ijk} = & (\nabla_l A_1) n_i n_j n_k n_l + (\nabla_l A_2) n_i n_j \delta_{kl} + (\nabla_l A_3) n_i n_k \delta_{jl} + (\nabla_l A_4) n_i n_l \delta_{jk} + (\nabla_l A_5) n_k n_l \delta_{ij} \\ & + (\nabla_l A_6) n_j n_k \delta_{il} + (\nabla_l A_7) n_j n_l \delta_{ik} + (\nabla_l A_8) \delta_{ij} \delta_{kl} + (\nabla_l A_9) \delta_{ik} \delta_{jl} + (\nabla_l A_{10}) \delta_{il} \delta_{jk} . \end{aligned} \quad (34)$$

Here $A_1 - A_{10}$ are functions of the order parameters S_2 and S_4 . In an equilibrium nematic phase the orientational order of NLC molecules is uniform in space and both order parameters are functions of temperature only. In other words, all $\nabla_l A_i$ vanish and so χ'_{ijk} does not affect the results discussed in the preceding sections. However, a different situation will occur at the NI phase transition. As discussed in Landau-de Gennes theory of NLC [18], heterophase fluctuations occur between phases and cause the nonuniformity of order parameters in space. Accordingly, in the vicinity of the NI-transition temperature T_c these fluctuations produce a sudden change in the values of the order parameters in a local region, from $S_2=S_4=0$ in the isotropic region to the nonvanishing S_2^N and S_4^N in the nematic one. So in Eq. (34) the terms

$$\nabla_l A_m(S_2, S_4) = \frac{\partial A_m}{\partial S_2} \nabla_l S_2 + \frac{\partial A_m}{\partial S_4} \nabla_l S_4 \quad (35)$$

may infinitely diverge at the interregion between the two phase regions. It is then easy to imagine that the APCT associated with the contribution of novel tensor χ' might display a critical behavior in the vicinity of T_c as shown in the experiment [see Fig. 4 of Ref. [1]]. In fact, the same critical phenomenon was also found in the LC Kerr effect [19], in which the electric field induces a birefringence near the NI transition

$$\Delta n = k E_{\text{app}}^2 , \quad (36)$$

where k is the Kerr constant and it increases sharply at

into each term of the right-hand side of Eq. (33) with every possible permutation. It is easily seen that the non-vanishing terms by this generation are identical to that of Eq. (19). So the general character of $B_1 - B_{16}$ should be similar to that of $A_1 - A_{10}$ except for a unit factor of e_{11} [see Eqs. (4.16) and (4.24) in Ref. [7]].

A statistical analysis [16] shows that all the A_i can always be expressed as linear functions of the order parameters S_2 and S_4 [the detailed definitions of which are given in Eq. (3.8) of Ref. [7]]. The same is true for $B_1 - B_{16}$. In LC theory [17], the dielectric anisotropy $\Delta\epsilon$ may be accepted as the macroexpression of order parameter, in particular of S_2 . Hence, the linear relation between B_i and $\Delta\epsilon$ is generally held.

B. Behavior in the NI transition

Similar to the Sec. V A, we now give a general consideration for the behavior of the APCT in the vicinity of the NI transition. By putting ∇_l on the left of A_i in Eq. (33), we generate in form a novel third-order tensor of the NOPF effect as

T_c . We believe the critical phenomenon in the Kerr effect is similar to that in the APCT.

C. Enhancement by exposure and dye doping

The above discussions have given a more complete answer to the phenomenological origin of the APCT. In this subsection, we supplement some applications of the present theory to the enhancement of the APCT effect.

In general, the conversion efficiencies of the LC photo-voltaic device reported [20,21] up to now are much lower than those of inorganic materials. One reason for this can be seen from the prediction of Eq. (30) that the bulk resistance R_0 is very large, i.e., the mobility of charge carriers is very low. This was true in our observation. We found that the 5CB sample in a fresh stage could not produce an obvious APCT effect (in this case its resistance is $R=200 \text{ M}\Omega$ [22]). We expose it with strong flash light for some time to decrease its resistivity [15]. After some exposure the APCT of this sample can be easily observed and its APCT is enhanced. For the example of $d=6.8 \mu\text{m}$ in thickness reported in our Letter [1], the final value of R may be estimated by the dark current $2 \text{ cm}^2 \times 0.5 \mu\text{A/cm}^2$ and the applied voltage $V_{\text{app}}=30 \text{ V}$. The result is $R=30 \text{ M}\Omega$.

A more efficient approach to enhancing the APCT effect of NLC was found by the theoretical prediction given in Eq. (28) related to the bulk contribution of the photorectification. The enhancement is clearly dominated by the absorption coefficient β . This motivated us to

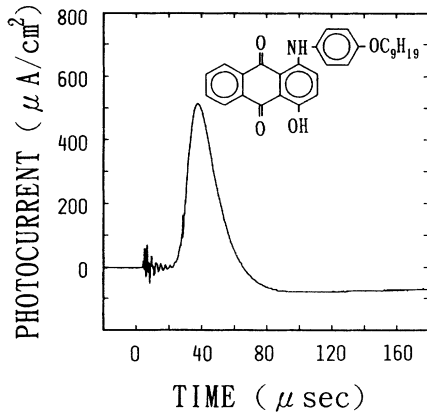


FIG. 6. Photoinduced current transients in a dye-doping NLC cell, with inset showing the molecular structure of the doping dye D16.

use dye doping, which serves for the enhancement of APCT in NLC because the dye doping can greatly enhance the light absorption of LC [13]. This experiment was carried out for the sample-doped 1.07 wt % dye D16

$$I_p = \frac{U_{OP}}{R_0 + R_e} \left[\frac{C_0 C_e (R_0 + R_e)}{C_0 + C_e} \frac{d}{dt} \delta \left(\frac{t}{\tau_0} \right) + \frac{(C_0^2 R_0 + C_e^2 R_e)(R_0 + R_e)}{(C_0 + C_e)^2 R_0 R_e} \delta \left(\frac{t}{\tau_0} \right) - \frac{(C_0 R_0 - C_e R_e)^2 (R_0 + R_e) \tau_0}{(C_0 + C_e)^3 R_0^2 R_e^2} \exp \left[-\frac{t}{\tau} \right] \right], \quad (37)$$

where

$$\tau = \frac{(C_0 + C_e) R_0 R_e}{R_0 + R_e}. \quad (38)$$

One finds that the first term, the differentiation of $\delta(t/\tau)$, gives a sharp up and down hedgehog shape in a front part of the APCT. In our present experimental setup, it is difficult to separate perfectly these noise and signal parts in a hedgehog shape of the APCT. Illuminating monochromatic light through an interference filter to a dye-doping sample described in Sec. V C, however, we have measured the APCT to make the hedgehog signal clear. The result is shown in Fig. 7. From this measurement the sharp up and down hedgehog shape of APCT is obvious. In an advanced experiment, the hedgehog signal predicted by Eq. (37) will be made more clear.

One possible reason for such a dye-doping effect is that the dye-doping cell has a larger value of bulk capacitance C_0 because we conjecture that the dye doping may also enhance the values of the dielectric constant. As reported earlier [23,24], optical reorientation in a dye-doping sample occurs at very low light-intensity levels. For example, the optical Fréedericksz transition occurs at 1.5 mW input power in homeotropic films of the impurity-host system using D82E63. This threshold value corresponds to the typical value of 100 mW observed in transparent nematic liquid crystals. It may be inferred that

[1-hydroxy-4-(4'-nonoxynilino)-anthraquinone] (see Appendix 8 of Ref. [15]) in 5CB. Without pretreatment of multiexposure, the dye-doping cell shows a great improvement in enhancement of APCT. From the measurement of the light energy, the enhanced ratio is estimated to be more than 10, as shown in Fig. 6. Furthermore, the dye doping also reduced the resistivity of the cell.

D. Hedgehog shape in APCT

The last problem is to discuss the "hedgehoglike" noise occurring in a front part of the APCT shape (see Fig. 2). A part of the hedgehog shape before the light pulse is apparently an electric noise induced by the discharge of the xenon lamp. However, a part of the hedgehog shape after the light pulse may not be noise but a real part of the APCT inclined in our presented theory. If we do not neglect the influence of the bulk capacitance C_0 in an equivalent circuit shown in Fig. 4(b), the complete form of APCT I_p will be given instead of Eq. (30) by

the dye-doping effect may be due to the increase of $\Delta\epsilon$ and/or the decrease of K [see Eq. (16)], although the authors of Refs. [23] and [24] did not claim these origins. In the absence of additional information, however, we cannot be sure of the inference and leave this as an open question.

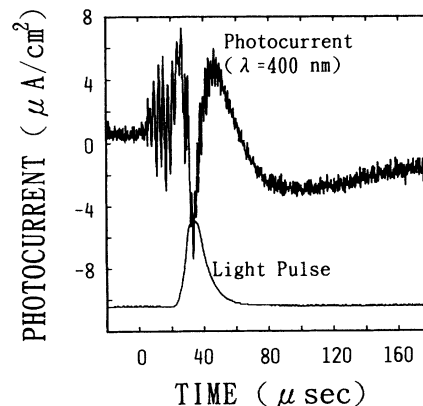


FIG. 7. Photoinduced current transient shape (hedgehog) for monochromatic light illumination of wavelength 400 nm in a dye-doping NLC cell. Because of the use of an interference filter, the intensity of APCT is weak.

VI. CONCLUSIONS

The mechanism of the anomalous photoinduced current transients in NLC has been made clear by the theoretical treatment based on a nonlinear optical Pockel's effect in an asymmetric cell induced by the Fréedericksz transition. The explicit expression is given for the photovoltaic emf in the case of the splay mode of NLC, including contributions both from molecular tilt in asymmetric way and bulk absorption of the light. With an equivalent circuit to account for the dc field-induced ion drift to electrodes, the obvious photocurrent formula is obtained and shows good agreement with experiment. The general behavior of nonlinear optical Pockel's coefficients is discussed with Landau-de Gennes theory. The greater part of the characteristics observed in our experiment have been well explained. The present theoretical prediction also motivates us to find two methods, exposure and dye doping, to enhance this novel optoelectric effect. These results suggest that the effect of the field-controlled photoinduced current transient with doping technique may change the application of LC from recent passive display style to the active information- and energy-conversion mode. This may be useful in a potential application to future optical and neural-network computers. Of course, in this study there remain many problems to be studied, e.g., the detailed mechanism for giving the quantitative values of NOPF coefficients $B_1 - B_{16}$ and the field dependence of the parameters of

the nonlinear circuit R_e , C_e , and so on. The former relates not only to physics but also to optochemistry and may be more difficult to deal with. The latter may be solved in physics but will be concerned with the nonlinear dynamics of both ions and LC. A program for the latter problem is in progress [25].

ACKNOWLEDGMENTS

The authors express their appreciation to Osaka Sangyo University and The Institute of Theoretical Physics, Academia Sinica, for their support of our joint research. The authors also would like to thank K. Hattori and H. Wakemoto of the Display Technology Research Laboratory, Matsushita Electric Industrial Co., Ltd., for the preparation of the samples. This work was supported in part by a Grant-in-Aid for Scientific Research from the Ministry of Education, Science and Culture of Japan, and Tateisi Science and Technology Foundation. We thank Dr. M. L. Du for his kind critical reading for our manuscript.

APPENDIX A: CONTRIBUTION OF FIELD GRADIENTS

By straightforward manipulations of Eq. (2.12) in Ref. [7], and Eqs. (8), (21), and (22) one can show the contribution of field gradients denoted in Eq. (3) by

$$\begin{aligned}
 P_z^{\text{NL}}(z, \omega=0) &= E_0^2 e^{-\beta(z+d/2)} \{ [iq(A_1 - A_1^*) - \beta(A_1 + A_1^*)] \cos^2\theta \sin^2\theta \cos^2\phi \\
 &\quad + [iq(A_3 - A_3^*) - \beta(A_3 + A_3^*)] \sin^2\theta + [iq(A_7 - A_7^*) - \beta(A_7 + A_7^*)] \cos^2\theta \cos^2\phi \\
 &\quad + [iq(A_9 - A_9^*) - \beta(A_9 + A_9^*)] \} , \tag{A1}
 \end{aligned}$$

where the A_j ($j=1,3,7,9$) are material constants. In more detail, the complex functions of ω_0 read as $A_j(0, -\omega_0, \omega_0)$ [see Eq. (2.13) of Ref. [7]]. Comparing Eq. (A1) with Eq. (27) one finds that this contribution can completely combine into the effect of U_{OP}^b and there is no need to consider it solely. In addition, as discussed in Sec. III C, the effect is related to the direction of the incident light and has been shown in experimental observation to be a weaker part in U_{OP} .

APPENDIX B: DERIVATION OF EQS. (30) AND (37)

To elucidate current transients in a linear circuit, one needs the use of the Laplace transform method. As a first step, we have to simplify the function of the light pulse intensity. The light pulse $f(t)$ shown in the illustrations does not seem to be well represented by δ functions. For the integral equality $\int I_0 \delta(t/\tau_0) dt = I_0 \tau_0 = \int f(t) dt$, however, the expediency of setting $f(t) = I_0 \delta(t/\tau_0)$ is

usual practice. Accordingly we make $U_{\text{OP}}(t) = U_{\text{OP}} \delta(t/\tau_0)$ and obtain its image function of the Laplace transform,

$$\hat{U}_{\text{OP}}(s) = \int_0^\infty e^{-st} U_{\text{OP}}(t) dt = U_{\text{OP}} \tau_0 . \tag{B1}$$

Considering the integral operation for the Laplace transform

$$\int_0^t F(t) dt \rightarrow \frac{1}{s} \hat{F}(s) \tag{B2}$$

in linear-circuit theory, the capacitance C can be seen as a resistance $\hat{C}(s) = 1/(Cs)$. Therefore, from the equivalent circuit shown in Fig. 4(b) (also set $C_0 = 0$), we then have the image function for $I_p(t)$,

$$\begin{aligned}\hat{I}_p(s) &= \hat{U}_{OP}(s) / \{R_0 + [1/(C_e s)]R_e / [R_e + 1/(C_e s)]\} \\ &= \frac{U_{OP}}{R_0} \{ \tau_0 - \tau_0 / [R_0 C_e (s + \tau)] \},\end{aligned}\quad (\text{B3})$$

where τ is given in Eq. (31). The original function of $\hat{I}_p(s)$ is just the result shown in Eq. (30). If $C_0 \neq 0$, the

last equation changes into

$$\begin{aligned}\hat{I}_p(s) &= \hat{U}_{OP}(s) / \{R_0 [1/(C_0 s)] / [R_0 + 1/(C_0 s)] \\ &\quad + R_e [1/(C_e s)] / [R_e + 1/(C_e s)]\}.\end{aligned}\quad (\text{B4})$$

This leads to the complete form of $I_p(t)$ shown in Eq. (37).

-
- [1] A. Sugimura, H. Sonomura, H. Naito, and M. Okuda, *Phys. Rev. Lett.* **63**, 555 (1989).
- [2] Ou-Yang Zhong-can, Sen Liu, and Xie Yu-zhang, *Phys. Rev. Lett.* **64**, 1475 (1990).
- [3] A. Sugimura, H. Sonomura, H. Naito, and M. Okuda, *Phys. Rev. Lett.* **64**, 1476 (1990).
- [4] A. Sugimura and Ou-Yang Zhong-can, in *Artificial Neural Networks*, edited by T. Kohonen, K. Mäkisara, O. Simula, and J. Kangas (Elsevier, Amsterdam, 1991), Vol. 2, p. 1525.
- [5] J. E. Bjorkholm and A. E. Siegman, *Phys. Rev.* **154**, 851 (1967).
- [6] V. Fréedericksz and V. Zolina, *Trans. Faraday Soc.* **29**, 919 (1933).
- [7] Ou-Yang Zhong-can and Xie Yu-zhang, *Phys. Rev. A* **32**, 1189 (1985).
- [8] H. Gruler, T. Scheffer, and G. Meier, *Z. Naturforsch. A* **27**, 966 (1972); H. Deuling, *Mol. Cryst. Liq. Cryst.* **19**, 123 (1972); H. Deuling and W. Helfrich, *Appl. Phys. Lett.* **25**, 129 (1974).
- [9] S. Lu and D. Jones, *Appl. Phys. Lett.* **16**, 484 (1970).
- [10] For example, see R. N. Thurston, *J. Appl. Phys.* **55**, 4145 (1984).
- [11] L. M. Blinov, *Electro-Optical and Magneto-Optical Properties of Liquid Crystals* (Wiley, New York, 1983), pp. 160 and 161.
- [12] F. C. Frank, *Discuss. Faraday Soc.* **25**, 19 (1958).
- [13] E. B. Priestley, P. J. Wojtowicz, and P. Sheng, *Introduction to Liquid Crystals* (Plenum, New York, 1975), pp. 157 and 119.
- [14] K. Sharp, S. T. Lagerwall, and B. Stebler, *Mol. Cryst. Liq. Cryst.* **60**, 215 (1980).
- [15] BDH catalog (British Drug House).
- [16] Xie Yu-zhang and Ou-Yang Zhong-can, *Commun. Theor. Phys. (Beijing)* **6**, 1 (1986).
- [17] P. G. de Gennes, *The Physics of Liquid Crystals* (Oxford University, London, 1974).
- [18] P. G. de Gennes, *Mol. Cryst. Liq. Cryst.* **12**, 193 (1971).
- [19] W. Helfrich and M. Schadt, *Phys. Rev. Lett.* **27**, 561 (1971); M. Schadt and W. Helfrich, *Mol. Cryst. Liq. Cryst.* **17**, 355 (1972).
- [20] H. Kamei, Y. Katayama, and T. Ozawa, *Jpn. J. Appl. Phys.* **11**, 1385 (1972).
- [21] K. Yoshino, S. Hisamitsu, and Y. Inuishi, *J. Phys. Soc. Jpn.* **32**, 867 (1972).
- [22] A. Sugimura, Y. Takahashi, N. Matsui, H. Sonomura, H. Naito, and M. Okuda, *Phys. Rev. B* **43**, 8272 (1991).
- [23] I. Janossy, A. D. Lloyd, and B. S. Wherrett, *Mol. Cryst. Liq. Cryst.* **203**, 77 (1991).
- [24] A. Sugimura and Ou-Yang Zhong-can, *J. Appl. Phys.* **70**, 2599 (1991).
- [25] A. Sugimura and Ou-Yang Zhong-can (unpublished).